Available online at www.sciencedirect.com
ScienceDirect
Polymer 48 (2007) 7604–7613
polymer
www.elsevier.com/locate/polymer

Controlled grafting from poly(vinylidene fluoride) microfiltration membranes via reverse atom transfer radical polymerization and antifouling properties

Yiwang Chen*, Qilan Deng, Jichun Xiao, Huarong Nie, Lichuan Wu, Weihua Zhou, Biwu Huang

Institute of Polymer Materials, School of Materials Science and Engineering, Nanchang University, Nanjing East Road 235, Nanchang, Jiangxi 330031, China

Received 3 August 2007; received in revised form 28 September 2007; accepted 26 October 2007
Available online 1 November 2007

Abstract

A reverse atom transfer radical polymerization (RATRP) with benzoyl peroxide (BPO)/CuCl/2,2-bipyridine (Bpy) was applied onto grafting of poly(methyl methacrylate) (PMMA) and poly(poly(ethylene glycol) methyl ether methacrylate) (PPEGMA) from poly(vinylidene fluoride) (PVDF) microfiltration (MF) membrane surfaces, including the pore surfaces. The introduction of peroxide and hydroperoxide groups onto the PVDF membranes was achieved by ultraviolet (UV) irradiation in nitrogen, followed by air exposure. RATRP from UV pretreated hydrophobic PVDF membranes was then performed for attaching well-defined homopolymer. The chemical composition of the modified PVDF membrane surfaces was characterized by attenuated total reflectance (ATR) FT-IR spectroscopy and X-ray photoelectron spectroscopy (XPS). The surface and cross-section morphology of membranes were studied by scanning electron microscopy (SEM). The pore sizes of the pristine PVDF and the PMMA grafted PVDF membranes were measured using micro-image analysis and process software. With increase of graft concentration, the pore size of the modified membranes decreased and became uniform. Kinetic studies of homogeneous (in toluene solution) system revealed a linear increase in molecular weight with the reaction time and narrow molecular weight distribution, indicating that the chain growth from the membrane surface was a ''controlled'' or ''living'' grafting process. The introduction of the well-defined PMMA on the PVDF membrane gave rise to hydrophilicity. Protein adsorption and protein solution permeation experiments revealed that the UV pretreated hydrophobic PVDF membrane subjected to surface-initiated RATRP of methyl methacrylate (MMA) and poly(ethylene glycol) methyl ether methacrylate (PEGMA) exhibited good antifouling property.
© 2007 Elsevier Ltd. All rights reserved.

Keywords: Poly(vinylidene fluoride); Ultraviolet irradiation; Microfiltration membrane

1. Introduction

Membrane filtration processes involving microfiltration (MF), ultrafiltration (UF) and nanofiltration (NF) are pressure-driven separation processes that are suited well for separating solution or suspension. They have been widely used in the field of environmental pollution treatment [1,2], seawater desalination [3,4], medicine [5,6], electronic and food technology [7] as well as in laboratory.

However, the low permeability or the reduction of the flux far below the theoretical capacity caused mainly by deposition and accumulation of submicron particles on the membrane surface has become one of the central problems in membrane filtration efficiency as it causes a reduction in productivity [8,9]. Most of organic membranes are treated with protein-containing solutions. Adsorption of proteins on microfiltration membranes is generally studied in terms of ''static adsorption,'' in which no pressure is applied. Therefore, protein fouling is believed to arise from the hydrophobic surfaces of traditional membranes, especially the surfaces of the pores [10]. The interest of the research, in particular during the last 20 years, was addressed to developing surface treatment

* Corresponding author. Tel./fax: +86 791 8336134.
E-mail address: ywchen@ncu.edu.cn (Y. Chen).

0032-3861/$ - see front matter © 2007 Elsevier Ltd. All rights reserved.
doi:10.1016/j.polymer.2007.10.043

methods to modify the membrane properties post-synthesis. These approaches have included coating and grafting techniques. In the former approach, the membrane is dipped in a solution containing polymers bearing the hydrophilic property [11,12]. But coating is generally not strong, especially some of the adsorbed protein will be desorbed during washing and operation. In the latter approach, grafting of hydrophilic species onto the surfaces of membranes has been used to efficiently improve permeation properties and reduce fouling [13,14]. Grafting can be achieved by surface graft of hydrophilic polymers or surface grafting copolymerization of the membrane with hydrophilic monomers or macromonomers in solutions [15,16]. Prior to the graft process, the membranes have to be activated by chemical [17], plasma [16,18–20], irradiation [21–23], and ozone [24,25] treatment to introduce the reactive groups on their surfaces.

Recently ''living'' polymerizations, including anionic [26] and cationic [27] polymerization, have been used to obtain graft copolymers with well-controlled structures [28–31]. Much attention also has been focused on controlled grafting from a solid surface [32–35]. Besides the stringent conditions required for ionic polymerizations, e.g., complete absence of water, they are limited by the scope of monomers that can be used. In contrast, controlled free radical polymerizations combine ease of polymerization and a large number of monomers capable of reaction. Controlled or living radical polymerizations combine the virtues of living ionic polymerization with the versatility and convenience of the free radical polymerization [36–38]. Successful examples of the living radical polymerization include nitroxide-mediated radical polymerization [39], atom transfer radical polymerization (ATRP) [40], and reversible addition-fragmentation chain transfer (RAFT) polymerization [41,42]. Preparation of well-defined polymer brushes via surface-initiated living radical polymerization has also received a considerable amount of attention in recent years [33,34,43–50]. The ''living''/controlled radical polymerization, atom transfer radical polymerization (ATRP), gives an efficient way to synthesize well-defined polymers. However, during the ATRP process, the halide species RX is usually toxic and the catalyst complex Mt^nL_m (where m is the number of ligands) is easily oxidized by the oxygen in air [51]. To overcome the drawbacks, a so-called reverse atom transfer radical polymerization (RATRP) has recently been explored. RATRP differs from normal ATRP in its initiation process, where a conventional radical initiator, such as BPO, is used instead of the organic halide initiator RX. A higher oxidation state transition metal catalyst complex $Mt^{n+1}XL_m$ is used instead of the lower oxidation state catalyst complex Mt^nL_m. So far, three types of efficient initiating systems for RATRP of monomers, AIBN/$CuCl_2$ (or $CuBr_2$)/2,2-bipyridine [52,53], BPO/CuCl/2,2-bipyridine [54] and AIBN/$FeCl_3$/PPh_3 [51], have been reported. ''Living''/controlled radical polymerizations of methyl methacrylate (MMA), methyl acrylate (MA), or styrene (St) were performed with the three systems.

Graft polymerization by the reverse atom transfer radical polymerization or other living polymerization processes, however, can be expected to simultaneously produce well-defined side chains, which, in turn, can be expected to facilitate the control of the pore size and the pore size distribution of the membrane. Graft polymerization via the traditional free radical process usually leads to uncontrolled size distribution. Surface-initiated ATRP from plasma-pretreated poly(vinylidene fluoride) membranes and surface-initiated RAFT-mediated polymerization from ozone-pretreated membranes were demonstrated for improving ion-exchange capacity and obtaining well-defined pore size distribution and responsibility, respectively [55–57]. The ''living''/controlled radical polymerization was also successfully used to modify fluorinated polyimide (FPI) [58] membrane and poly(2,6-dimethylphenylene oxide) (PPO) [59] membrane.

Poly(vinylidene fluoride) (PVDF) membranes, as a promising membrane material, has many unique properties including excellent process ability, chemical resistance, well-controlled porosity, and good thermal property [60,61]. Therefore, its membranes are widely used in microfiltration and ultrafiltration processes. However, the potential application of PVDF membranes in aqueous solution separation is limited by the hydrophobic nature of their surfaces, especially the surfaces of the pores [10]. Surface modification is expected to bring desired changes in hydrophilicity to PVDF membranes without altering the bulk properties. As we know, adsorption and permeation properties of porous membranes can be changed by the addition of polymeric layers onto their active surface [62]. For instance, a hydrophilic surface coating on a porous membrane is expected to reduce protein binding and increase flux.

In our previous study, PMMA was grafted by the surface-initiated free radical polymerization from the peroxide initiators generated by UV irradiation on PVDF surface followed by air exposure [63]. A goal of this work was to examine whether RATRP could be used to simultaneously change the membrane functionality, pore size, and pore size distribution in rational ways. Polymerization time was used as the independent variable to manipulate the amount of grafted poly(methyl methacrylate) on the UV pretreated hydrophobic PVDF membrane. By using a traditional radical initiator, peroxide generated by UV irradiation on hydrophobic PVDF membrane followed by air exposure, RATRP of methyl methacrylate from UV pretreated hydrophobic PVDF membrane was carried out under homogeneous conditions. Results showed that the membrane hydrophilicity, protein fouling resistance and protein permeability increased with increase of the graft polymerization time. It was important that a membrane with an initially larger pore size and broad pore size distribution has a smaller pore size and narrower pore size distribution following graft polymerization.

2. Experimental

2.1. Materials

Hydrophobic and hydrophilic poly(vinylidene fluoride) (PVDF) membranes (Millipore Durapore®, 0.45 μm pore

size, 125 μm thickness, of 25 mm diameter) were purchased from Millipore Inc., which are commercially named HVHP and HVLP, respectively.

Methyl methacrylate (MMA) monomer was washed with 5% NaOH and doubly distilled water, dehydrated by CaH_2 overnight, and then distilled under reduced pressure distillation. The purified MMA was stored in an argon atmosphere at −10 °C. Poly(ethylene glycol) methyl ether methacrylate (PEGMA) macromonomer ($M_n = 300$) was passed through the inhibitor remover column to remove the inhibitors and then stored in clean vessels at −10 °C. Toluene was distilled over CaH_2 before use. Benzoyl peroxide (BPO) in chloroform was recrystallized with methanol and stored at −15 °C. Copper(I) chloride (CuCl) was purified according to procedures described in the literature [35]. 2,2-Bipyridine (Bpy) was used without further purification.

2.2. UV irradiation pretreatment of PVDF membrane

The UV irradiation system with a CHG-200 photochemical reactor was manufactured by Aobodi Photoelectronic Technology Coop. of Peking Normal University in China. The reactor was equipped with 1800 mW/cm^2 high-pressure Hg lamp and the irradiation source was filtered with 297 nm filter. The PVDF membrane was placed in a Pyrex tube. After purging with purified nitrogen for about 30 min, the Pyrex tube was sealed with a silicon rubber stopper at room temperature. All UV-induced reactions were carried out at a constant temperature of 28 °C. A typical treatment time of 1 h was used. After the UV irradiation, the UV pretreated PVDF membranes were subsequently exposed to the atmosphere for about 10 min to affect the formation of peroxide and hydroperoxide species. The dependence of peroxide concentration on the UV irradiation pretreatment time under the same experimental conditions had been reported earlier [63]. The active species, such as peroxide and hydroperoxide, on the membrane surface were used for the subsequent surface-initiated reverse atom transfer radical polymerization (RATRP).

2.3. Surface-RATRP of MMA and PEGMA from UV pretreated PVDF membrane

Polymerization was carried out in toluene as solvent and using methyl methacrylate as the monomer. Both monomer MMA (2 mL, 18.7 mmol) and solvent toluene (6 mL) were stirred and degassed with argon for 20 min. Then CuCl (5.97 mg, 0.06 mmol), Bpy (18.72 mg, 0.12 mmol), BPO (14.54 mg, 0.06 mmol) and the UV irradiation-treated and air-exposed PVDF membrane were added into the solution. The reaction flask was sealed and placed in a 60 °C oil bath for a predetermined period of time. After the reaction, the PVDF membrane with grafted poly(methyl methacrylate) (PMMA) brushes was removed from the solution and washed thoroughly by stirring for 12 h in an excess acetone and doubly distilled water to remove any residual monomer and ‘‘free’’ PMMA homopolymer, if any. The so-modified membrane was dried in a vacuum oven until the weight kept unchanged. The ‘‘free’’ PMMA formed in solution by the free initiator was recovered by precipitating into excess methanol, filtered, and dried under a vacuum oven. The dried polymer was weighed to obtain a monomer conversion. The process of UV pretreatment and the surface-initiated RATRP of MMA from PVDF membrane are shown schematically in Fig. 1.

For the preparation of poly(poly(ethylene glycol) methyl ether methacrylate) (PPEGMA) brushes from the UV pretreated PVDF membranes, both monomer PEGMA (2.5 mL, 7.5 mmol) and solvent (doubly distilled water) (2 mL) were stirred and degassed with argon for 20 min. Then CuCl (8.96 mg, 0.09 mmol), Bpy (28 mg, 0.18 mmol), BPO (21.81 mg, 0.09 mmol) and the UV irradiation-treated and air-exposed PVDF membrane were added into the solution. The reaction flask was sealed and placed in a 60 °C oil bath for 7 h. After the reaction, the PVDF membranes with grafted PPEGMA brushes were removed from solution and washed thoroughly by stirring for 12 h in an excess doubly distilled water to remove any residual monomer and ‘‘free’’ homopolymer.

2.4. Characterization

Attenuated total reflectance (ATR) FT-IR spectra of the surface functionalized films were obtained from a Shimadzu IRPrestige-21 spectrophotometer using a ZnSe prism with an incident angle of 60°. Each spectrum was collected by cumulating 160 scans at a resolution of 4 cm^{-1}. A contact angle measurement JC2000A was used to measure static water contact angles of the polymer films at 25 °C and 60% relative humidity using a sessile drop method. For each angle reported, at least five sample readings from different surface locations were averaged. The angles reported were reliable to ±2°.

The chemical composition of the pristine and the functionalized PVDF membranes was determined by X-ray photoelectron spectroscopy (XPS). The XPS measurements were performed on a Kratos AXIS Ultra spectrometer using a monochromatic Al Kα X-ray source (1486.71 eV photons) at a constant dwell time of 100 ms and a pass energy of 40 eV. The samples were mounted on the standard sample studs by means of double-sided adhesive tapes. The core-level signals were obtained at

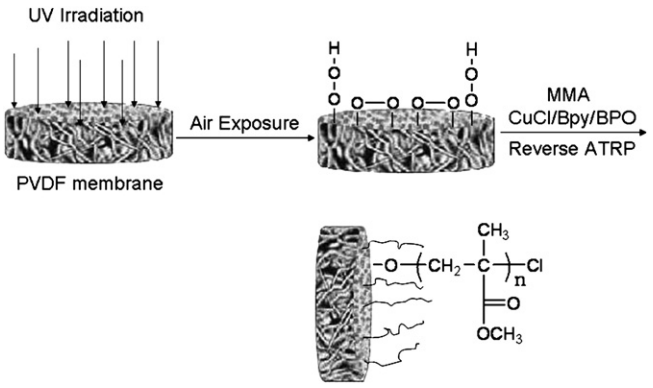

Fig. 1. Schematic diagram illustrating the process of UV irradiation pretreatment followed by surface-initiated reverse atom transfer radical polymerization of MMA from the hydrophobic PVDF membrane.

a photoelectron takeoff angle (α, measured with respect to the sample surface) of 90°. The X-ray source was run at a reduced power of 225 W (15 kV and 15 mA). The pressure in the analysis chamber was maintained at 10^{-8} Torr or lower during each measurement. All binding energies (BE's) were referenced to the C 1s hydrocarbon peak at 284.8 eV. Surface elemental stoichiometries were determined from the spectral area ratios, after correcting with the experimentally determined sensitivity factors, and were reliable to within ±10%. The elemental sensitivity factors were determined using stable binary compounds of well-established stoichiometries.

Size-exclusion chromatography (SEC) in chloroform was carried out on a Waters Breeze GPC system consisting of a Rheodyne injector, a 1515 Isocratic pump and a Waters 2414 differential refractometer. SEC was performed in chloroform. Each sample (200 μL of about 3% w/v solution) was injected through Styragel HT3 and HT4 columns (19 mm × 300 mm) at 40 °C and flow rate of 1.0 mL/min to separate MW ranging from 10^2 to 10^6.

The surface morphology of the MF membranes was studied by scanning electron microscopy (SEM), using a Hitachi S-4300 electron microscope. The membranes were mounted on the sample studs by means of double-sided adhesive tapes. A thin layer of platinum was sputtered on the sample surface prior to the SEM measurement. The SEM measurements were performed at an accelerating voltage of 5 kV. The pore sizes of the pristine hydrophobic PVDF and the modified PVDF membranes were directly measured from images for obtaining average value by using micro-image analysis and process software. For cross-sectional view studies, the membrane was fractured under liquid nitrogen. A thin layer of platinum was sputtered onto the cross-sectional surface prior to the SEM measurement.

2.5. Protein fouling measurement

To investigate the antifouling properties of the modified PVDF membranes, the membranes were first exposed to solutions containing bovine serum albumin (BSA). The membranes were hydrated initially by immersion in methanol, followed by immersion in distilled water. The membranes were subsequently washed with the phosphate buffer saline (0.01 M PBS, pH 7.4) for 1 h before being incubated in PBS containing 2 mg/mL of BSA for 24 h at room temperature. After removal from the protein solution, they were washed for 5 min in three batches of PBS, followed by three batches of distilled water. Finally, samples were dried in a vacuum oven at room temperature. The surface coverage of BSA was quantified by XPS, using the nitrogen signal associated with BSA. Survey spectra were run in the binding energy range of 0–1000 eV. The near-surface atomic compositions of the membranes were determined from the numerically integrated core-level spectral area ratios, corrected with the respective elemental sensitivity factors. Permeation experiments were performed at room temperature (25 °C) and 0.09 MPa transmembrane pressure using as stirred microfiltration cell (Model 8003, Millipore, USA). The concentration of the protein (BSA) solution in PBS (pH 7.4) was 1 mg/mL. The effective membrane area was 0.95 cm^2. The flux was calculated from the weight of the solution permeated per unit time and per unit area of the membrane surface.

3. Results and discussion

Polymer brushes on PVDF membrane were synthesized according to the reaction sequence shown schematically in Fig. 1. Prior to the surface-initiated reverse atom transfer radical polymerization (RATRP), the PVDF film was subjected to UV irradiation in nitrogen for 1 h, followed by air exposure for 10 min, to form the peroxide and hydroperoxide initiator species on the PVDF surface. The formation and coverage of peroxide species on PVDF surfaces has been ascertained by XPS and determination quantitatively with 2,2-diphenyl-1-picrylhydrazyl (DPPH) in previous work [63]. Polymer brushes were prepared by surface-initiated RATRP of methyl methacrylate (MMA) from the peroxide initiators on the PVDF surfaces.

3.1. Surface-initiated RATRP from the UV pretreated PVDF membrane

The advantage of RATRP over other living polymerization, such as anionic and cationic polymerization, is the tolerance for various functionalities in the monomers, leading to polymers with functionalities along the chains, similar to ATRP. The new molecular functionalities can be incorporated onto the activated PVDF membrane via RATRP. Therefore, the physicochemical properties of the PVDF membrane can be tuned by the choice of a variety of vinyl monomers. As the model monomer, MMA was selected. The poly(methyl methacrylate) (PMMA) grafted PVDF membrane could be effective in preventing protein adsorption and fouling. A biocompatible PVDF membrane with PMMA brushes can be used in the PVDF membrane-based bioreactor.

RATRP differs from conventional ATRP in its initiation step that the active radical abstracts a halogen atom from the catalyst and forms the dormant halide species and the reduced transition metal species activator [64]. In this process, conventional radical initiator (e.g., 2,2′-azobisisobutyronitrile) is used instead of the organic halide initiator RX, and CuX_2 (X = Cl and Br) and 2,2-bipyridine (Bpy) are used as a catalyst and a complexing ligand [65]. Xia and Matyjaszewski reported a RATRP of styrene with BPO initiator. The presence of $CuBr_2$ could not control the radical polymerization of styrene. However, catalyzed by CuBr, the living radical polymerization went smoothly [66]. The coordination of the bidentate nitrogen ligand to Cu(I) increases the solubility of the inorganic salt and facilitates the redox reaction between CuCl and benzoyl peroxide (BPO). The radical was generated through the electron transfer from Cu(I) complexed by Bpy to the BPO, and initiated the radical polymerization of MMA. Then, Cu(II) complexed by Bpy reacts reversibly with growing radicals and gains electron from the growing radicals, a reversible activation of the resulting alkyl chlorides occurs, and the polymerization proceeds via the ATRP mechanism. An equilibrium

is established where the dormant polymer chains are reversibly activated via a halogen atom transfer reaction. Therefore, this article uses a RATRP of MMA from peroxide species with BPO as an initiator and CuCl/Bpy complex as a catalyst. The radical from peroxide and hydroperoxide covalently bonded on PVDF membrane can reversibly react with $CuCl_2$ which is produced from redox reaction of CuCl by BPO in solution. No polymer brushes on PVDF membrane were observed while RATRP of MMA from UV pretreated PVDF membrane was carried out without BPO. The experiment excluded the possibility of direct ATRP from secondary fluoride of PVDF main-chain in this reaction condition. For removing "free" PMMA blending on membrane, the PMMA grafted PVDF membrane was thoroughly washed with acetone and distilled water.

The polymer brushes can be prepared from UV irradiation-treated and air-exposed PVDF membrane via RATRP of appropriate functional monomers. The new molecular functionalities can be incorporated onto the activated fluoropolymer surfaces. Therefore, the physicochemical properties of the PVDF membrane can be tuned by the choice of a variety of vinyl monomers [67]. As the model monomer, MMA was selected. The presence of grafted PMMA on UV pretreated PVDF membrane is ascertained by XPS analysis. The C 1s core-level spectrum of the non-treated hydrophobic PVDF membrane consists of two peak components of about equal integral area with BE at 286.2 eV for the CH_2 species and at 290.9 eV for the CF_2 species (Fig. 2). Peak component at 284.8 eV is attributable to the C–H species from the internal reference for XPS scan. Only peaks 286 and 688 eV, attributable to C 1s and F 1s, are observed in the XPS wide-scan spectrum of the non-treated hydrophobic PVDF membrane. The XPS wide-scan spectrum of PMMA grafted PVDF membrane consists of peaks at 286, 531, and 688 eV, attributable to C 1s, O 1s, and F 1s, respectively. The C 1s core-level spectra of the PMMA grafted PVDF membrane can be curve-fitted with five peak components having BE's at about 284.8, 286.2, 286.6, 288.9, and 290.9 eV, attributable to the Neutral C, CH_2, C–O, O–C=O, and CF_2 species, respectively. The [C–O]/[O–C=O] ratios, obtained from XPS analysis, are in fairly good agreement with the respective theoretical ratios. In addition, the CF_2 peak component associated with the PVDF membrane persists in the curve-fitted C 1s core-level spectra of the PMMA grafted PVDF membrane, but presents a lower area in comparison to the CH_2 component. The graft concentration of the PMMA brushes grafted from the PVDF membrane can be derived from the O–C=O peak component to the CF_2 peak component. With the increase of RATRP time, thus increase of PMMA concentration on the membrane, the [O–C=O]/[CF_2] ratio from C 1s core-level spectra and [O]/[F] ratio from wide-scan spectra of PMMA grafted PVDF membrane increase (Fig. 3).

The presence of PMMA and PPEGMA brushes from the PVDF membrane is ascertained also by ATR FT-IR spectra. The ATR FT-IR spectra of the PMMA and PPEGMA grafted PVDF membrane reveal the appearance of the absorption band at 1730 cm^{-1}, attributable to the stretching of ester carbonyl group, as shown in Fig. 4. The variations in graft concentration (RATRP time) are reflected in the changes in ratio of the intensity of the absorption band at 1730 cm^{-1} to that of the absorption band at 1400 cm^{-1}. The absorption band at 1181 cm^{-1} in ATR FT-IR spectra of PPEGMA grafted PVDF membrane was sharper than that of PMMA grafted PVDF membrane due to vibration absorption of C–O–C.

The variation in water contact angle for the PVDF membrane with PMMA brushes indicates that the hydrophilicity of the PVDF membrane can be easily tuned, according to RATRP time. The contact angle of the non-treated hydrophobic PVDF membrane is about 124°. When grafted with a PMMA brushes, the PVDF membrane becomes more hydrophilic and the contact angle decreases with increase of graft concentration (relative to RATRP time), as shown in Fig. 5. The water contact angle of the UV pretreated PVDF membrane subjected to RATRP of MMA for 10 h decreases to 94°, while the water contact angle of the PPEGMA grafted PVDF membrane reduces to 87°.

Additional evidence for the controlled polymerization was provided by analysis of the "free" PMMA formed in solution from the free initiator. Fig. 6a shows the linear relationship between $\ln([M_0]/[M])$ and polymerization time, where $[M_0]$ is the initial monomer concentration and $[M]$ is the monomer concentration at time t. The result indicates that the concentration of the growing species remains constant and kinetics are first-order. Fig. 6b shows the relationship between molecular weight (M_n) of the "free" PMMA formed in solution and the conversion of the MMA monomer. The number-average

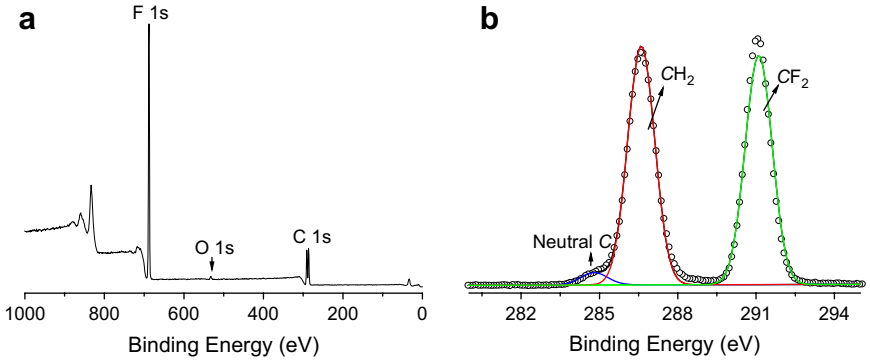

Fig. 2. XPS wide-scan (a) and C 1s core-level spectrum (b) of the pristine hydrophobic PVDF membrane.

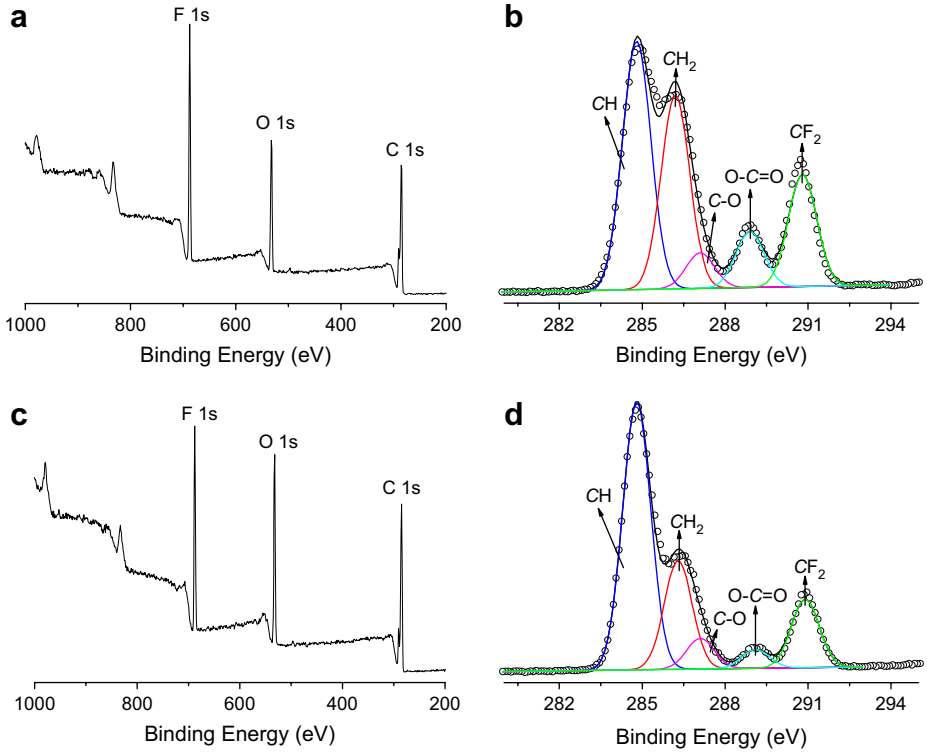

Fig. 3. XPS wide-scan and C 1s core-level spectra of the UV pretreated hydrophobic PVDF membrane subjected to RATRP of MMA for polymerization of (a, b) 3 h and (c, d) 16 h. Reaction conditions: [MMA]/[CuCl]/[Bpy]/[BPO] = 312/1/2/1, [MMA] = 2.34 M, solvent toluene, temp 60 °C.

molecular weight of the "free" PMMA increases linearly with the increase in monomer conversion. The polydispersity index (M_w/M_n) of the free PMMA remains at around 1.2–1.3 throughout the reaction. Although the exact molecular weight of the polymer grafted from the PVDF membrane is not known, its molecular weight is expected to be proportional to that of the polymer formed in the solution [41]. The kinetic results indicate that the processes of the surface-initiated RATRP of MMA are consistent with a "controlled" process.

3.2. Surface morphology of the pristine and modified PVDF membranes

Fig. 7 shows SEM images at (a) magnification of 5000× for the pristine hydrophobic PVDF membrane, and (b) SEM image at magnification of 5000× for the UV pretreated

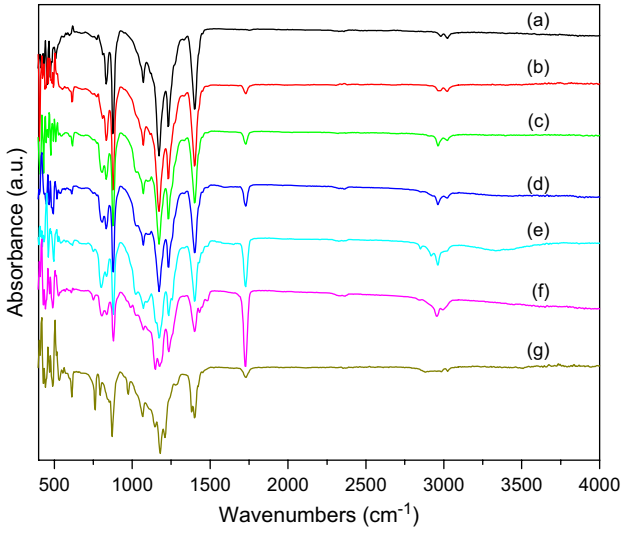

Fig. 4. ATR FT-IR spectra of (a) the pristine hydrophobic PVDF MF membrane, and the PMMA grafted PVDF MF membranes for (b) 0.5 h, (c) 1 h, (d) 5 h, (e) 10 h, and (f) 16 h, and (g) the PPEGMA grafted PVDF MF membrane for 7 h. Reaction conditions: [MMA]/[CuCl]/[Bpy]/[BPO] = 312/1/2/1, [MMA] = 2.34 M, solvent toluene, temp 60 °C. Reaction conditions: [PEGMA]/[CuCl]/[Bpy]/[BPO] = 83/1/2/1, [PEGMA] = 1.66 M, solvent (doubly distilled water), temp 60 °C.

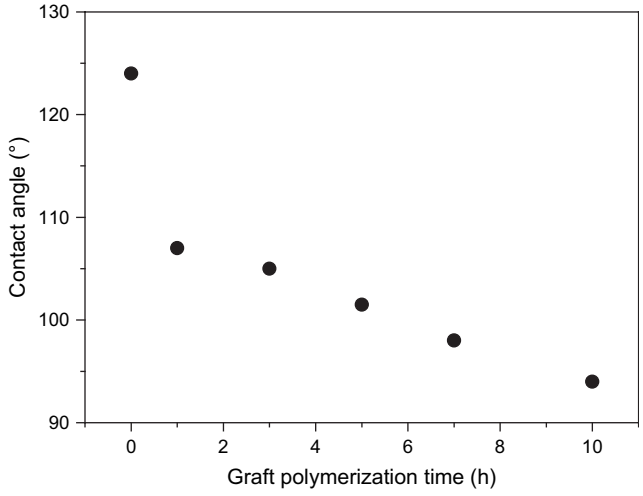

Fig. 5. Variation of water contact angle of PVDF-*g*-PMMA membrane on the corresponding surface-initiated RATRP graft time. Reaction conditions: [MMA]/[CuCl]/[Bpy]/[BPO] = 312/1/2/1, [MMA] = 2.34 M, solvent toluene, temp 60 °C.

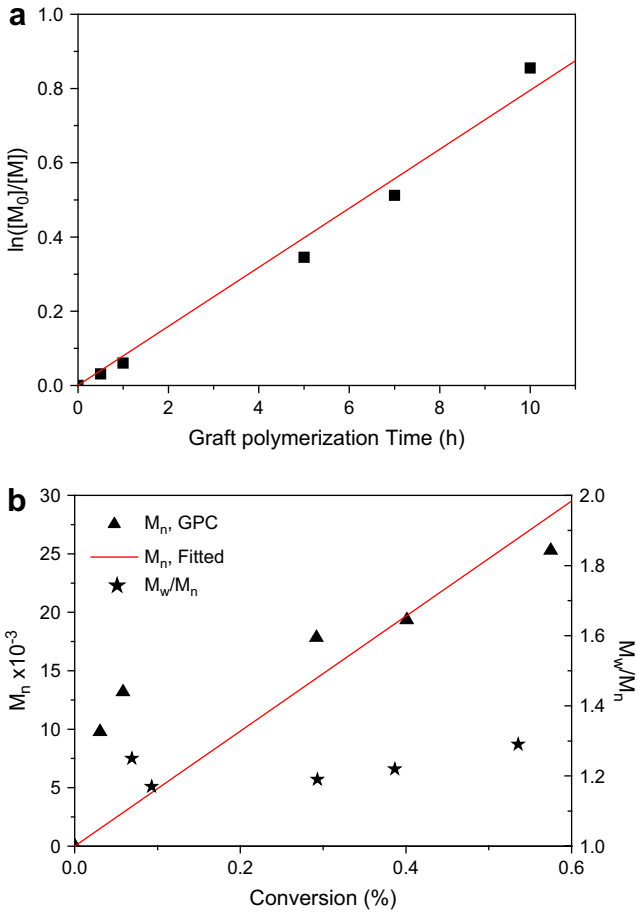

Fig. 6. Relationship (a) between $\ln([M_0]/[M])$ and the polymerization time and (b) between M_n of "free" PMMA and the monomer conversion in polymerization solution. Reaction conditions: [MMA]/[CuCl]/[Bpy]/[BPO] = 312/1/2/1, [MMA] = 2.34 M, solvent toluene, temp 60 °C.

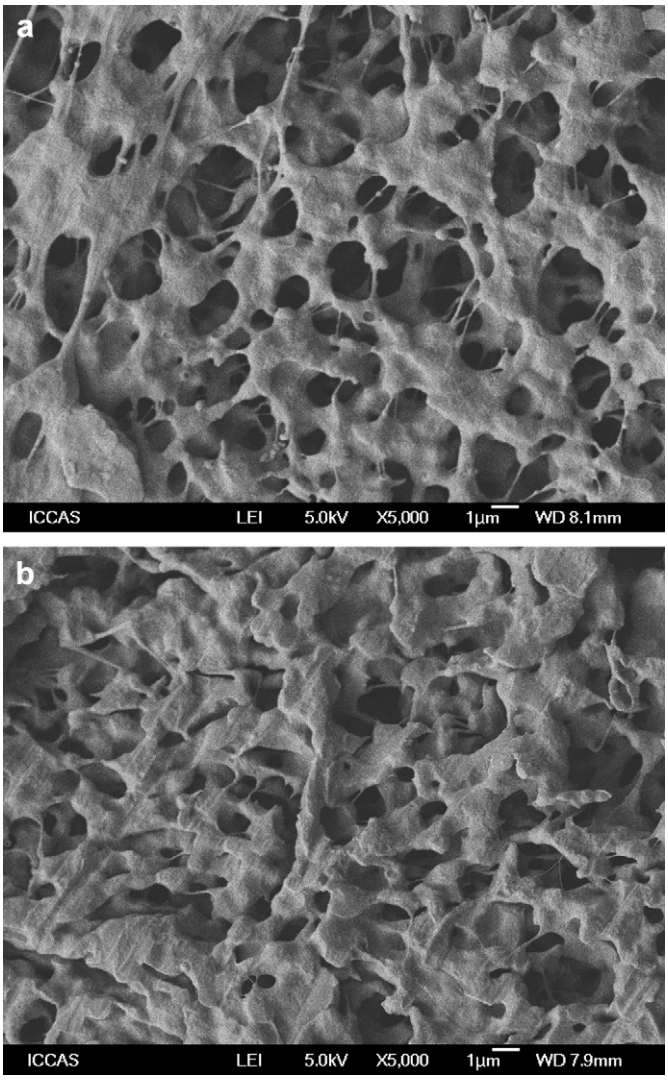

Fig. 7. SEM images of (a) the pristine hydrophobic PVDF membrane and (b) the UV pretreated hydrophobic PVDF subjected to RATRP of MMA for 16 h.

hydrophobic PVDF subjected to RATRP of MMA for 16 h. The non-treated hydrophobic PVDF membrane used in this study shows relatively very high porosity and small pore size. The modified PVDF membrane exhibits that the membrane fibers have grown thicker and the pore sizes have become more uniform and smaller. With the increase of the grafting degree (graft polymerization time), the membrane pores were plugged. The non-treated hydrophobic and modified PVDF membranes show a homogenous morphology in their cross-sections as well on the surfaces. The cross-sectional views of the modified membranes in Fig. 8 show that the polymer was grafted on the membrane outer surface and also from the pore surfaces within the bulk of the membranes. Peroxide species were generated from not only membrane outer surface but also pore surfaces because UV irradiation could reach pore surfaces through membrane pores without limitation of penetration depth. The penetration depth of UV depends on the UV power. In this work, the thickness of membranes (125 μm) is far less than the penetration depth of UV. Therefore polymer brushes occur throughout pore surfaces of the membrane.

Micro-image analysis and Process software were used to determine the membrane surface pore size and pore size distributions of the non-treated hydrophobic PVDF and modified PVDF membranes by surface-initiated RATRP (Table 1). By changing polymerization time, the average surface pore diameter decreased from 1.42 to 0.75 μm. Equally important, the pore size distribution became narrower following surface-initiated polymerization.

3.3. Permeation and antifouling properties

The presence of PMMA chains on the membrane surface, including the pore surface, imparts significant resistance to protein adsorption. The surface composition of the membranes after exposure to a 2 mg/mL BSA solution for 24 h was analyzed by XPS. The relative amount of BSA adsorbed onto the surface can be simply expressed as the [N]/[F] ratio. The dependence of the [N]/[F] ratio on the PMMA polymer graft concentration (graft polymerization time via RATRP of MMA from UV pretreated hydrophobic PVDF membrane) on the PVDF membrane is summarized in Fig. 9. The error of experimental values is less than 3% due to XPS error. In

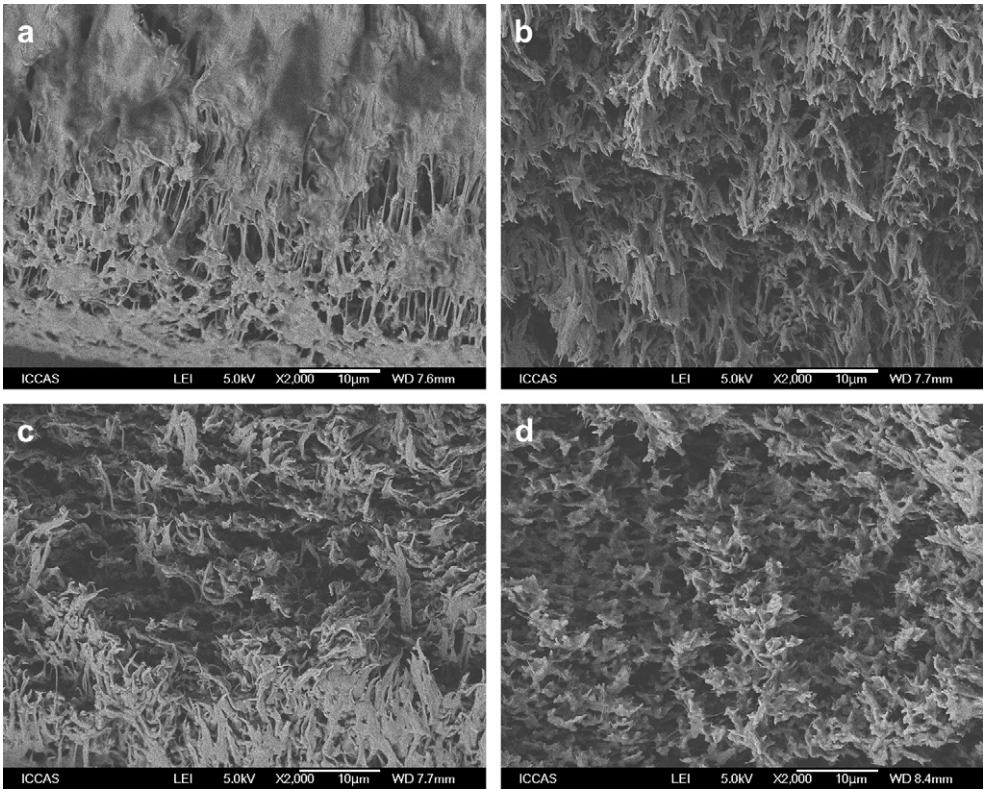

Fig. 8. SEM cross-sectional images of (a) the pristine hydrophobic PVDF membrane, and the UV pretreated hydrophobic PVDF membranes subjected to RATRP of MMA for (b) 1 h, (c) 5 h and (d) 16 h.

comparison to non-treated hydrophobic PVDF membranes, the modified PVDF membranes show substantially enhanced resistance to BSA adsorption. The level of BSA adsorption for the UV pretreated PVDF membrane subjected to RATRP of MMA for 16 h is less than 27% of that of non-treated hydrophobic PVDF membrane. The determination of elemental amount by XPS only characterized static protein adsorption of membrane surface due to limitation of the XPS penetration depth. Even though radio-labeled or fluorescent-labeled protein could be applied to quantify bulk protein adsorption of membrane, the permeation experiment of protein solution through membranes was a qualitative method to characterize bulk protein adsorption.

Pure water permeation measurement was carried out to characterize the permeation properties of the modified membranes. The water permeability of the non-treated hydrophobic PVDF membrane was also measured and compared with those of the modified ones. Fig. 10 shows the results of the water flux curves for the non-treated and grafted PVDF membranes. The non-treated hydrophobic PVDF membrane cannot let water flow across in our case. It can be seen that, with increase of MMA grafting degree (graft polymerization time), the water flux increases. The water flux of grafted PVDF membrane by RATRP of MMA for 16 h after UV pretreatment increases to 0.29 $cm^3/(cm^2\ s)$. Generally, pore size and surface

Table 1
Pore size measurement of the pristine hydrophobic and the UV pretreated hydrophobic PVDF membranes subjected to RATRP of MMA

	Graft time (h)	Pore size (μm)		
		Mean	Max	Min
1	0	1.42	3.33	0.52
2	1	1.20	3.12	0.27
3	5	1.05	2.61	0.24
4	10	0.81	2.31	0.22
5	16	0.75	2.22	0.19

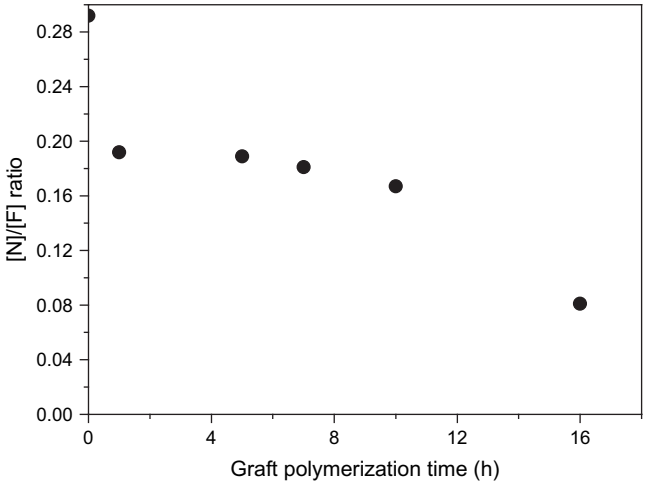

Fig. 9. Dependence of the extent of BSA adsorption (expressed as the [N]/[F] ratio) on the graft polymerization time via RARTP from UV pretreated hydrophobic PVDF membranes.

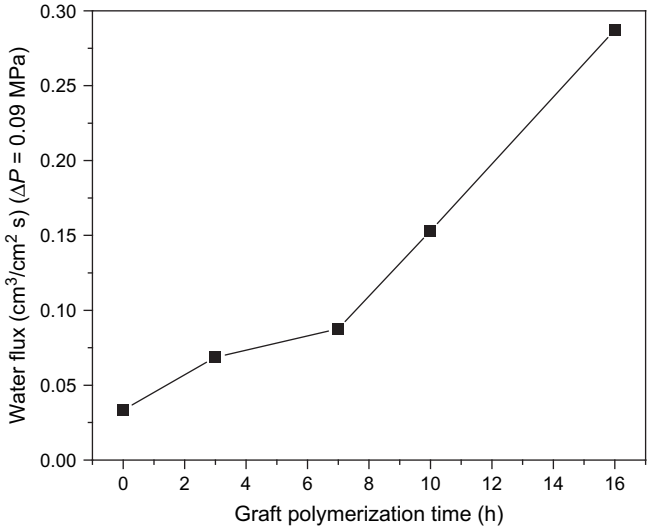

Fig. 10. Water fluxes through the pristine hydrophobic PVDF membrane and the UV pretreated hydrophobic PVDF membranes subjected to RATRP for different time.

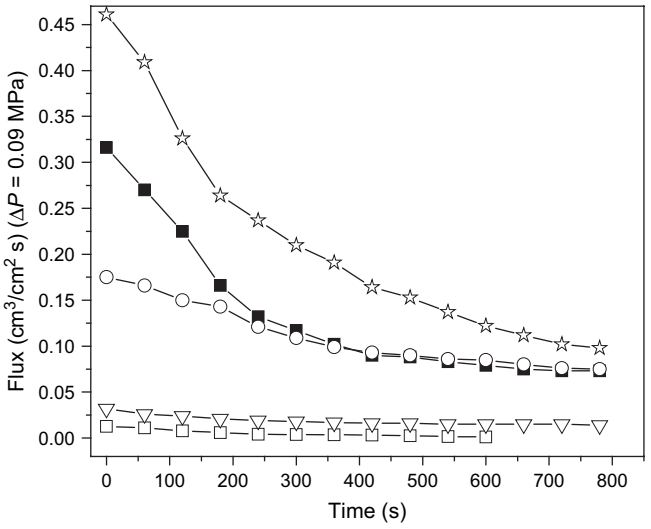

Fig. 11. Decline in the permeation rate of the bovine serum albumin solution (1 mg/mL) as a function of time through the Millipore hydrophilic (solid square) and hydrophobic (open square) PVDF membranes and the UV pretreated hydrophobic PVDF membranes subjected to RATRP of MMA for 3 h (open triangle) and 16 h (open circle) and subjected to RATRP of PEGMA for 7 h (open star).

hydrophilicity are the two parameters which affect water flux most. When the grafting degree is low, the surface hydrophilicity is the dominant factor and the water flux enhances with the increase of grafting degree accordingly despite pore blocking. However, pore blocking becomes the leading factor at higher grafting degree and causes the decline of the water flux. In this study, decline of the water flux has not been observed yet when graft polymerization time is lower than 16 h. The results indicated that the graft polymerization time of 16 h gives rise to insufficient high grafting degree at which pore blocking becomes the leading factor to cause the decline of the water flux.

The protein (BSA) solution flux data of Fig. 11 allow a comparison of the antifouling property of the present modified PVDF membrane with the commercial PVDF membranes. Commercially hydrophilic and hydrophobic PVDF membranes of comparable pore dimensions from Millipore were used in the permeation experiment. The UV pretreated PVDF membrane followed by RATRP of MMA thus exhibits a better antifouling property in the dynamic fouling process than that of the non-treated hydrophobic PVDF membrane. The antifouling ability of the grafted PVDF membrane by RATRP after UV pretreatment is comparable to that of the commercial "low-protein-binding" Millipore hydrophilic membrane. When subjected to prolonged flux, the grafted PVDF membrane by RATRP for 16 h after UV pretreatment exhibits even better fouling resistance than the commercial hydrophilic PVDF membrane. On the other hand, the flux of the protein solution through the commercial hydrophobic PVDF membrane became too low to be measured accurately after 600 s. As we know, PEGMA is a better antifouling monomer. The PVDF membrane was modified by grafting PEGMA polymer via RATRP process for 7 h after UV pretreatment according to similar procedures as grafting PMMA. A significant increase in BSA solution flux through the PVDF membrane grafted PEGMA polymer indicated that the PVDF membrane grafted PEGMA polymer by RATRP for 7 h after UV pretreatment has better antifouling property than the commercial hydrophilic PVDF membrane.

4. Conclusions

Poly(methyl methacrylate) (PMMA) and poly(poly(ethylene glycol) methyl ether methacrylate) (PPEGMA) could be covalently immobilized or grafted onto the PVDF microfiltration membrane surfaces, including the pore/channel surfaces, by the simple process of reverse atom transfer radical polymerization (RATRP) from UV pretreated PVDF membrane. The grafting polymer brushes from UV pretreated PVDF membranes by RATRP was reproducible process. Using this technique, membrane pore size and pore size distribution could be adjusted using polymerization time as the independent variable. It was found that the water flux through the membrane increased with increasing PMMA graft concentration (graft polymerization time). The decrease of the water contact angles and the increase of the pure water flux for the modified PVDF membrane indicate the improvement of the surface hydrophilicity by the grafting of PMMA. Protein adsorption and permeation flux experiments revealed that the grafted PVDF membrane by RATRP of MMA after UV pretreatment exhibited good antifouling property. The PPEGMA grafted PVDF membrane is more effective in preventing protein fouling than PMMA grafted PVDF membrane due to high hydrophilicity of PEGMA.

Acknowledgements

Financial support for this work was provided by the National Natural Science Foundation of China (50403016 and

50773029), the Program for New Century Excellent Talents in University (NCET-06-0574), the Natural Science Foundation of Jiangxi Province (520044), and the Program for Innovative Research Team of Nanchang University.

References

[1] Singh AK, Gupta VK, Gupta B. Anal Chim Acta 2007;585:171–8.
[2] Wever HD, Weiss S, Reemtsma T, Vereecken J, Müller J, Knepper T, et al. Water Res 2007;41:935–45.
[3] Macedonio F, Profio GD, Curcio E, Drioli E. Desalination 2006;200: 612–4.
[4] Yu DG, Jou C, Lin WC, Yang MC. Colloids Surf B 2007;54:222–9.
[5] Park S, Jang HJ, Choi YS. J Mater Sci Mater Med 2007;18:475–82.
[6] Liu YF, Yu QC, Wu YH. J Phys Chem Solids 2007;68:201–5.
[7] Howe JK, Ishida PK, Clark MM. Desalination 2002;147:251–5.
[8] Zhao CS, Zhou XS, Yue YL. Desalination 2000;129:107–23.
[9] Uyama Y, Kato K, Ikada Y. Adv Polym Sci 1998;137:1–39.
[10] Kim KJ, Fane AG, Fell CJD. Desalination 1998;70:229–49.
[11] Brink LES, Elbers SJG, Robbertsen T, Both P. J Membr Sci 1993;76: 281–91.
[12] Ulbricht M, Matuschewski H, Oechel A, Hicke HG. J Membr Sci 1996; 115:31–47.
[13] Ulbricht M, Belfort G. J Membr Sci 1996;111:193–215.
[14] Wang Y, Kim JH, Choo KH, Lee YS, Lee CH. J Membr Sci 2000;169: 269–76.
[15] Ulbricht M, Richau K, Kamusewitz H. Colloid Surf A 1998;138:353–66.
[16] Iwata H, Matsuda T. J Membr Sci 1988;38:185–99.
[17] Brynaert JM, Jongen N, Dewez JL. J Polym Sci Part A Polym Chem 1997;35:1227–35.
[18] Wang PW, Tan KL, Kang ET, Neoh KG. J Adhes Sci Technol 2002;16: 111–27.
[19] Xie R, Chu LY, Chen WM, Xiao W, Wang HD, Qu JB. J Membr Sci 2005;258:157–66.
[20] Yang Q, Xu ZK, Dai ZW, Wang JL, Ulbricht M. Chem Mater 2005;17: 3050–8.
[21] Ulbricht M, Riedel M, Marx U. J Membr Sci 1996;120:239–59.
[22] Liu F, Zhu BK, Xu YY. Appl Surf Sci 2006;253:2096–101.
[23] Liu Q, Zhu ZY, Yang XM, Chen XL, Song YF. Rad Phys Chem 2007;76:707–13.
[24] Ying L, Zhai GQ, Winata AY, Kang ET, Neoh KG. J Colloid Interf Sci 2003;265:396–403.
[25] Ying L, Kang ET, Neoh KG, Kato K, Iwata H. J Membr Sci 2004;243: 253–62.
[26] Lu HL, Chung TC. J Polym Sci Part A Polym Chem 1999;37:4176–83.
[27] Kennedy P, Vidal A. J Polym Sci 1975;13:1765–75.
[28] Wang XS, Luo N, Ying SK. Polymer 1999;40:4515–20.
[29] Miwa Y, Yamamoto K, Sakaguchi M, Shimada S. Macromolecules 1999; 32:8234–6.
[30] Beers KL, Gaynor SG, Matyjaszewski K, Sheiko SS, Möller M. Macromolecules 1998;31:9413–5.
[31] Hawker CJ, Wooley KL. Science 2005;3098:1200–5.
[32] Yamamoto S, Ejaz M, Tsujii Y, Fukuda T. Macromolecules 2000;33: 5602–7.
[33] Yamamoto S, Ejaz M, Tsujii Y, Matsumoto M, Fukuda T. Macromolecules 2000;33:5608–12.
[34] Husseman M, Malmström EE, McNamara M, Mate M, Mecerreyes D, Benoit DG, et al. Macromolecules 1999;32:1424–31.
[35] Matyjaszewski K, Miller PJ, Shukla N, Immaraporn B, Gelman A, Luokala BB, et al. Macromolecules 1999;32:8716–24.
[36] Huang X, Wirth MJ. Macromolecules 1999;32:1694–6.
[37] Coessens V, Pintauer T, Matyjaszewski K. Prog Polym Sci 2001;26: 337–77.
[38] Pyun J, Matyjaszewski K. Chem Mater 2001;13:3436–48.
[39] Hawker CJ, Bosman AW, Harth E. New polymer synthesis by nitroxide mediated living radical polymerization. Chem Rev 2001;101: 3661–88.
[40] Matyjaszewski K, Xia J. Chem Rev 2001;101:2921–90.
[41] Drockenmuller E, Li LYT, Ryu DY, Harth E, Russell TP, Kim HC, et al. J Polym Sci Part A Polym Chem 2005;43:1028–37.
[42] Hao XJ, Nilsson C, Jesberger M, Stenzel MH, Malmström E, Davis TP, et al. J Polym Sci Part A Polym Chem 2004;42:5877–90.
[43] Baum M, Brittain WJ. Macromolecules 2002;35:610–5.
[44] Yu WH, Kang ET, Neoh KG, Zhu SP. J Phys Chem B 2003;107:10198–205.
[45] Edmondson S, Huck WTS. J Mater Chem 2004;14:730–4.
[46] Granville AM, Boyes SG, Akgun B, Foster MD, Brittain WJ. Macromolecules 2004;37:2790–6.
[47] Feng W, Brash J, Zhu S. J Polym Sci Part A Polym Chem 2004;42: 2931–42.
[48] Reddy SK, Sebra RP, Anseth KS, Bowman CN. J Polym Sci Part A Polym Chem 2005;43:2134–44.
[49] Liu T, Casado-Portilla R, Belmont J, Matyjaszewski K. J Polym Sci Part A Polym Chem 2005;43:4695–709.
[50] Wang YP, Pei XW, He XY, Lei ZQ. Eur Polym J 2005;41:737–41.
[51] Moineau G, Dubois P, Jerome R, Senninger T, Tessie P. Macromolecules 1998;31:545–7.
[52] Wang JS, Matyjaszewski K. Macromolecules 1995;28:7901–10.
[53] Xia JH, Matyjaszewski K. Macromolecules 1997;30:7692–6.
[54] Wang WX, Yan DY, Jiang XL, Detrembleur C, Lecomte P, Jerome R. Macromol Rapid Commun 2001;22:439–43.
[55] Singh N, Husson SM, Zdyrko B, Luzinov I. J Membr Sci 2005;262: 81–90.
[56] Chen YW, Ying L, Yu WH, Kang ET, Neoh KG. Macromolecules 2003; 36:9451–7.
[57] Ying L, Yu WH, Kang ET, Neoh KG. Langmuir 2004;20:6032–40.
[58] Chen YW, Chen L, Nie HR, Kang ET, Vora RH. Mater Chem Phys 2005;94:195–201.
[59] Cho CG, Jang HY, You YG, Li GH, An SG. High Perform Polym 2006;18:579–91.
[60] Wang LD, Li K, Teo WK. J Membr Sci 1999;163:211–20.
[61] Li K. Chem Eng Technol 2002;25:203–6.
[62] Zeman LJ. J Membr Sci 1983;15:213–30.
[63] Deng QL, Chen YW, Sun W. Surf Rev Lett 2007;14:23–30.
[64] Li P, Qiu KY. Polymer 2002;43:3019–24.
[65] Limer, Haddleton DM. Eur Polym J 2006;42:61–8.
[66] Xia JH, Matyjaszewski K. Macromolecules 1999;32:5199–202.
[67] Tan KL, Woon LL, Wong HK, Kang ET, Neoh KG. Macromolecules 1993;26:2832–6.